Surface and thickness profile measurement of a transparent film by three-wavelength vertical scanning interferometry

Katsuichi Kitagawa

Toray Engineering Co. Ltd., 1-1-45 Oe, Otsu 520-2141, Japan (katsuichi.kitagawa@nifty.com)

Received April 25, 2014; revised June 11, 2014; accepted June 16, 2014;
posted June 17, 2014 (Doc. ID 210882); published July 9, 2014

We have developed a novel areal film thickness and topography measurement method using three-wavelength interferometry. The method simultaneously estimates the profiles of the front and back surfaces and the thickness distribution of a transparent film by model-based separation of two overlapped signals in an interferogram. The validity of the proposed method is demonstrated using computer simulations and actual experiments.

OCIS codes: (120.3180) Interferometry; (120.3940) Metrology; (240.0310) Thin films; (310.6860) Thin films, optical properties.
http://dx.doi.org/10.1364/OL.39.004172

In the industry, optical interferometry is widely applied for surface profile measurement as a noncontact and nondestructive method for quickly and accurately measuring the profiles of microscopic surfaces. However, its application to transparent thin films has been limited because it is difficult to obtain an exact surface profile measurement if the surface to be measured is covered with a transparent film. This is because the interference beam coming from the back surface of the film creates disturbance.

To solve this problem, we developed algorithms to separate the interference signal of the front surface from that of the back surface in vertical scanning white-light interferometry [1–3]. If the thickness of a transparent film is greater than the coherent length, two peaks of reflection corresponding to the front and back surfaces appear on the interferogram, and they can be easily separated. However, separating the peaks is difficult if the thickness is less than 1 μm and the two peaks overlap each other. To overcome this problem, researchers have proposed various methods using the Fourier transform [4–6] or the wavelength scanning technique [7,8]. However, these techniques suffer from some disadvantages, such as complex computation algorithm, necessity of an *a priori* knowledge of the dispersive film index, and requiring specialized hardware.

Thickness profile measurement is also of great importance in industry, for example, the measurement of various types of thin film layers on substrates of semiconductors or flat-panel display devices. There are several different techniques used to measure these films, of which the most widely used are reflection spectrophotometry and ellipsometry. However, most of these techniques are limited to single-point measurement. To obtain an areal thickness profile, it is necessary to mechanically scan the sample or the sensing device. Another limitation inherent in these techniques is their large spot sizes. For example, spectrophotometers are limited to spot sizes of a few micrometers or greater because of available light budgets.

To resolve these drawbacks, we developed a new approach called the separation of overlapped sinusoidal signals (SOSS) algorithm that estimates the profiles of the front and back surfaces and the thickness distribution of a transparent film by using multiwavelength vertical scanning interferometry.

In our technique, a three-wavelength interferometric imaging system [9–11] is used, which comprises a three-wavelength (B, G, R) illumination system and a color camera (Fig. 1). The transmittance of the multibandpass filter is shown in Fig. 2. The spectral sensitivity of the camera is shown in Fig. 3. Using this system, we can obtain three interferograms with different wavelengths simultaneously [Fig. 4(a)]. Unfortunately, the spectral response curves of the camera overlap slightly, as shown in Fig. 3; therefore, there is cross talk in the BGR color signals. This problem can be solved using a cross talk compensation algorithm, as reported in [9–11].

Because the bandwidth of each illumination light is narrow enough, the interferograms can be expressed as the sum of two sinusoidal signals, one corresponding to the front surface and one to the back surface:

$$g(i,j) = a(j) + b_1(j)\cos\left[\frac{4\pi(z(i)-z_1)}{\lambda(j)}\right] + b_2(j)\cos\left[\frac{4\pi(z(i)-z_2)}{\lambda(j)}\right], \quad (1)$$

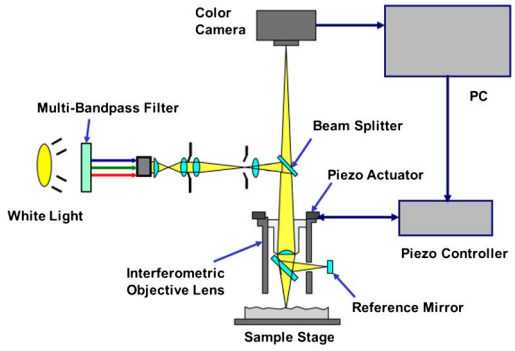

Fig. 1. System configuration for three-wavelength vertical scanning interferometry.

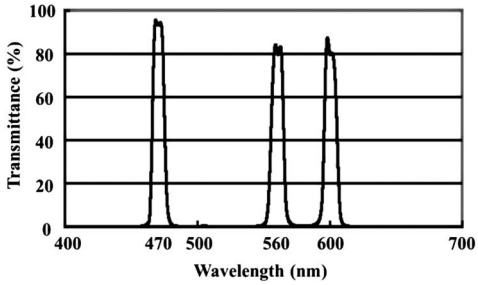

Fig. 2. Transmittance of multibandpass filter.

where $g(i,j)$ is the intensity at frame $i(i = 1, 2, \ldots, N)$ and wavelength $j(j = \mathrm{B}, \mathrm{G}, \mathrm{R})$; $a(j)$ is the average value; $b_1(j)$ and $b_2(j)$ are the modulations of the waveform of the front surface and the back surface, respectively; $z(i)$ is the reference mirror scanning position; z_1 and z_2 are the heights of the front surface and the back surface, respectively; and $\lambda(j)$ is the wavelength. The unknown parameters $a(j)$, $b_1(j)$, $b_2(j)$, z_1, and z_2 are estimated using the following least-square fitting equation:

$$F = \sum_{j=1}^{3} \sum_{i=1}^{N} [g(i,j) - g_{i,j}]^2, \tag{2}$$

where $g(i,j)$ is the model intensity, and g_{ij} is the observed intensity.

Please note that our model neglects multiple reflections because the error caused by it is negligibly small in typical films; e.g., the relative error of the subsurface reflection intensity is 0.8% in SiO_2-Si structure. Even if the error cannot be neglected, we can use our algorithm by using the model, which considers the multiple reflections.

Let us consider the necessary conditions to obtain the unknown parameters. The total number of parameters is 11. However, there are nine meaningful parameters among three interferograms, because a sinusoidal wave has three meaningful parameters: the bias, amplitude, and phase. Therefore, this least-square fitting problem cannot be solved. To make it solvable, let us note that the ratio of the modulations $b_1(j)$ and $b_2(j)$ is dependent on the refractive indices of the film and substance, and it can be expressed as follows:

$$\alpha = \frac{(n-1)(n+1)}{4n} \sqrt{\frac{(n+n_B)^2 + \kappa_B^2}{(n-n_B)^2 + \kappa_B^2}}, \tag{3}$$

where α is the ratio of the modulations; n and n_B are the refractive indices of the film and substrate, respectively; and κ_B is the extinction coefficient of the substrate.

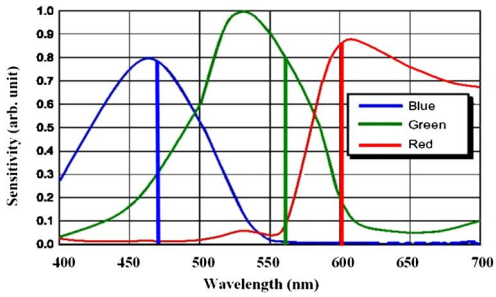

Fig. 3. Spectral sensitivity of camera for the three wavelengths used.

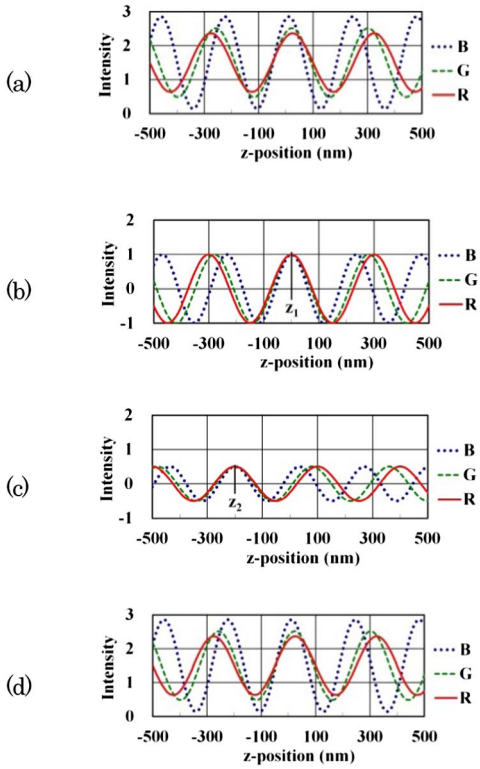

Fig. 4. Waveforms in computer simulation: (a) synthesized data, (b) separated surface signals, and (c) separated back surface signals, and (d) fitted signals.

Because the refractive indices n and n_B are almost constant in the wavelength range of 470–600 nm for most film-substrate materials used in industry, we can assume that α is independent of the wavelength. Thus, $b_1(j)$ can be expressed as follows:

$$b_1(j) = \alpha b_2(j). \tag{4}$$

Using Eqs. (1) and (4), we obtain

$$g(i,j) = a(j) + \alpha b_2(j) \cos\left[\frac{4\pi(z(i) - z_1)}{\lambda(j)}\right] + b_2(j) \cos\left[\frac{4\pi(z(i) - z_2)}{\lambda(j)}\right]. \tag{5}$$

The number of unknown parameters is reduced to nine, that is, $a(j)$, $b_2(j)$, z_1, z_2, and α. Thus, the least-square fitting problem becomes solvable.

Please note that the number of unknown parameters can be reduced to eight if the refractive indices are known and α is obtained by Eq. (3). In this case, the assumption of constant α is unnecessary.

Using the obtained z_1 and z_2, the thickness t and the back surface physical height z_b can be calculated as follows:

$$t = (z_1 - z_2)/n, \tag{6}$$

$$z_b = z_1 - t. \tag{7}$$

To find solutions to the nonlinear least-square problem, we use an iterative technique that requires initial

estimates that allow us to search for the minimum matching error point. Because the model function of Eq. (5) contains a cosine function, the error function has many local minima. Therefore, it is essential to make good initial estimates.

In this Letter, the initial estimates are calculated as follows. $a(j)$ is the average of the observed intensity values, and $b_2(j)$ is the range of observed intensity values divided by $2(1+\alpha)a(j)$. α is the theoretical value given by Eq. (3). To estimate z_1 and z_2, we estimate the peak position z_0 of the white-light interferogram that is approximated by the sum of the three interferograms. Using z_0 and the estimated thickness t_0, the initial estimates of z_1 and z_2 are calculated as follows.

If $\alpha >= 1$, that is, if the front surface signal is stronger than the back surface signal, then $z_1 = z_0$ and $z_2 = z_0 - t_0$. If $\alpha < 1$, that is, if the back surface signal is stronger than the front surface signal, then $z_1 = z_0 + t_0$ and $z_2 = z_0$.

To verify the proposed algorithm, we designed a computer simulation. A set of theoretical three-wavelength interferograms was obtained using the parameters shown in the "True" column of Table 1. The wavelengths are 470 nm (B), 560 nm (G), and 600 nm (R). The synthesized signals are shown in Fig. 4(a). All of the computations were performed in MS Excel using a Windows PC. The initial guess values were set as shown in the "Initial" column of Table 1.

The results are presented in Table 1. The parameters and heights were correctly estimated. The separated waveforms and the fitted model waveform are shown in Figs. 4(b)–4(d).

For the actual experiments, we wrote a software program in the programming language C to implement the algorithm on the Windows PC. The nonlinear least-squares equation was solved using the Davidon–Fletcher–Powell method [12]. To avoid unbalanced error estimation among the wavelengths, we normalized the observed intensity data so that all data were between 0 and 2, as shown in Fig. 7(a).

As mentioned before, we needed to avoid the local minima problem. Accordingly, we used the multistart method, which finds the global minimum by solving the least-squares equation with multiple initial values. We performed the same numerical simulation described above, except for various initial thickness values. The results are shown in Fig. 5. When the initial estimate error is between −90 and +180 nm, the thickness is correctly estimated around 200 nm. Otherwise, it converges to a local minimum near the initial estimate. Please note that

Table 1. Results of Computer Simulation

Variables	True	Initial	Estimated	Error
a(B)	1.50	1.57	1.50	0.00
a(G)	1.50	1.42	1.50	0.00
a(R)	1.50	1.44	1.50	0.00
b(B)	0.50	0.45	0.50	0.00
b(G)	0.50	0.34	0.50	0.00
b(R)	0.50	0.29	0.50	0.00
α	2.00	2.50	2.00	0.00
z(1)	0.00	50.00	0.00	0.00
z(2)	−200.00	−250.00	−200.00	0.00

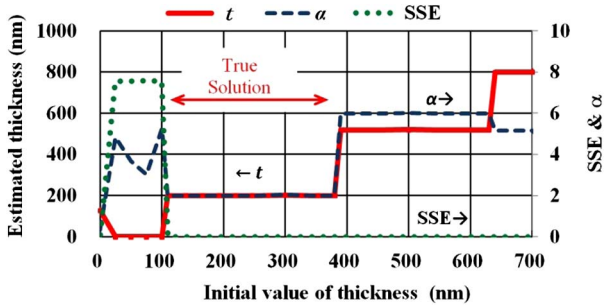

Fig. 5. Effect of the initial value of thickness on the results of computer simulation.

the sum of the squared error (SSE) exhibits little difference among the local minima. Therefore, we selected the global minimum by comparing the obtained value of α with its initial value, which was usually set as the theoretical value given by Eq. (3).

In our experiments, a thin film thickness step gauge was tested using silicon dioxide ($n = 1.46$) on silicon substrates with thicknesses of 100 and 300 nm (Fig. 6). The vertical scanning speed was 150 nm/s, and the sampling interval was 10 nm.

Figure 7 shows the results at the center position of the image. The observed data after the cross-talk compensation and normalization are shown in Fig. 7(a). The separated and fitted signals are shown in Figs. 7(b)–7(d). The obtained parameters were $z_1 = 628$ nm, $z_2 = 481$ nm, and $\alpha = 0.45$. Using these values, the thickness of 101 nm was obtained.

Figure 8 shows 3D views of the obtained front and back surfaces and thickness profiles of the whole area. Note that the back surface is correctly measured to be flat in spite of the film thickness step. The areal average thicknesses were 294 and 102 nm. These agree well with the nominal values. The total calculation time for 160×120 pixels was approximately 72 s on the Windows PC (3.4 GHz Intel Core i7-2600 CPU). Because the calculation is pixel-independent, the speed would be very much improved by a parallel processing technique.

In conclusion, we proposed a new interferometric profiling technique called the SOSS algorithm that enables us to estimate the profiles of the front and back surfaces and the thickness distribution of a transparent film by separating two overlapped signals in an interferogram. In our technique, a three-wavelength interferometric imaging system is used, comprising a three-wavelength (B, G, R) illumination system and a color camera. Using this optical system, three interferograms with different wavelengths can be obtained simultaneously. On the basis of the observed interferogram data, we can estimate the unknown parameters, including the front and back

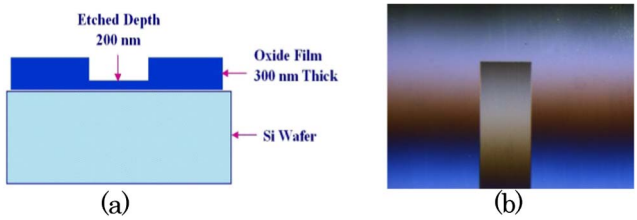

Fig. 6. Test target in the actual experiment: (a) cross section and (b) one of the captured interference images.

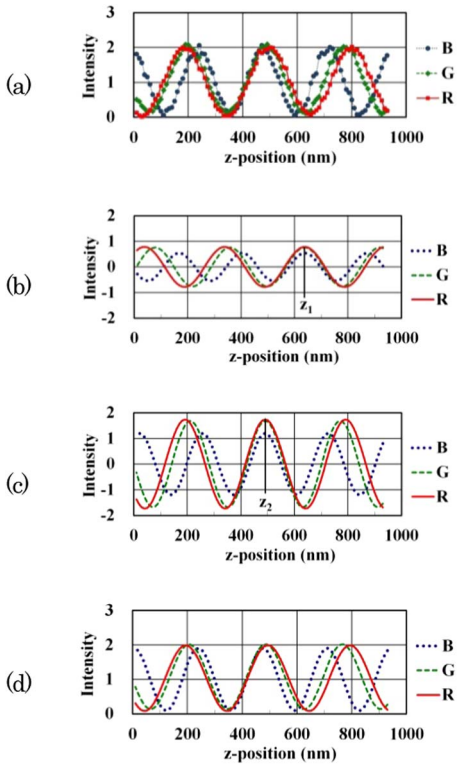

Fig. 7. Waveforms at the central pixel in the actual experiment: (a) observed signals, (b) separated surface signals, (c) separated back surface signals, and (d) fitted signals.

surface heights, using the least-squares fitting method with some assumptions to reduce the number of the unknown parameters. The proposed method has been validated by computer simulations and experiments. The most significant feature of this technique is that we can easily obtain the necessary hardware by inserting a multibandpass filter in the path of illumination and replacing the monochrome camera with a color camera in the conventional white-light interferometric profiler.

References

1. K. Kitagawa, Proc. SPIE **6375**, 637507 (2006).
2. K. Kitagawa, Proc. SPIE **6716**, 671607 (2007).

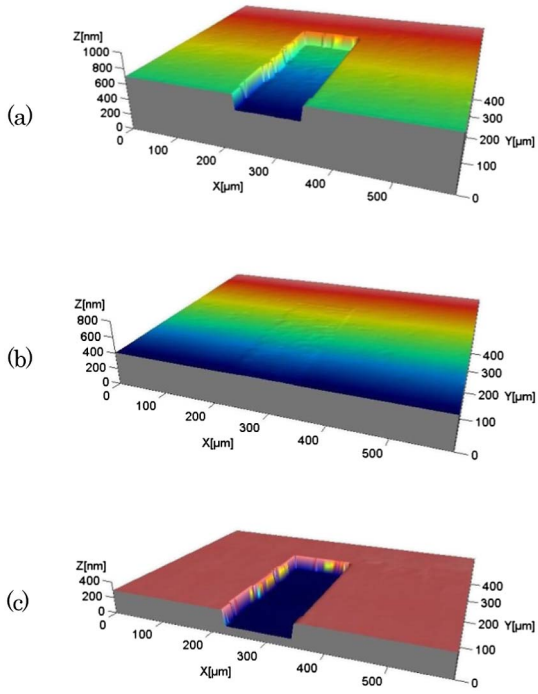

Fig. 8. Results of the actual experiment: (a) estimated front surface profile; (b) estimated back surface profile; and (c) estimated thickness profile.

3. K. Kitagawa, in *Handbook of Optical Metrology—Principles and Applications*, T. Yoshizawa, ed. (CRC Press, 2009), pp. 677–691.
4. S. W. Kim and G. H. Kim, Appl. Opt. **38**, 5968 (1999).
5. D. Mansfield, Proc. SPIE **7101**, 71010U (2008).
6. P. J. de Groot and X. C. de Lega, Proc. SPIE **7064**, 70640I (2008).
7. D. Kim, S. Kim, H. Kong, and Y. Lee, Opt. Lett. **27**, 1893 (2002).
8. H. Akiyama, O. Sasaki, and T. Suzuki, Opt. Express **13**, 10066 (2005).
9. K. Kitagawa, Int. J. Optomechatron. **4**, 136 (2010).
10. K. Kitagawa, J. Electron. Imaging **21**, 021107 (2012).
11. K. Kitagawa, Appl. Opt. **52**, 1998 (2013).
12. R. Fletcher and M. J. D. Powell, Comput. J. **6**, 163 (1963).